

FPU β model: Boundary Jumps, Fourier's Law and Scaling

Kenichiro Aoki^a and Dimitri Kusnezov^b

^a*Dept. of Physics, Keio University, 4-1-1 Hiyoshi, Kouhoku-ku, Yokohama 223-8521, Japan*

^b*Center for Theoretical Physics, Sloane Physics Lab, Yale University, New Haven, CT 06520-8120*
(October 30, 2018)

We examine the interplay of surface and volume effects in systems undergoing heat flow. In particular, we compute the thermal conductivity in the FPU β model as a function of temperature and lattice size, and scaling arguments are used to provide analytic guidance. From this we show that boundary temperature jumps can be quantitatively understood, and that they play an important role in determining the dynamics of the system, relating soliton dynamics, kinetic theory and Fourier transport.

Transport in low dimensional systems has enjoyed renewed interest due to new efforts to understand why some theories have a bulk limit for transport coefficients and others do not [1–5]. The FPU β model, in particular, provides a classic example of a system with no bulk limit [4,5]. Steady state transport is typically generated by imposing boundary conditions on surfaces of the system of interest, that provide the necessary behavior, such as shearing, heat flow and so forth. A physical and ubiquitous feature of these boundary-driven non-equilibrium steady states are surface discontinuities in certain observables [6]. In fluids that are being sheared, a slip velocity develops at the boundary reflecting the fact that the fluid just inside the system does not move with the same velocity as the walls. In systems undergoing heat flow, as in the FPU model we study here, a ‘surface resistance’ or boundary jump in temperature develops. We will show that these surface effects can be quantitatively understood, and that the interplay of surface and volume effects can be used to define dynamical regimes, characterized by different scaling properties. To provide a more complete picture, we compute both the temperature and size dependence of the thermal conductivity κ , as well as the speed of sound and other kinetic theory quantities. From the behavior of κ , we will also see that the presence of a constant thermal gradient does not guarantee that Fourier’s law, specifically the linear relation between the heat flow J and ∇T , $J = -\kappa\nabla T$, is valid. (We refer to the relation $J = -\kappa\nabla T$ as Fourier’s law, even in the absence of the bulk limit.) The role of solitons can also be understood.

Heat flow is generated by applying hot (T_2^0) and cold (T_1^0) sources to the different boundaries of the system. However, in general there will be a mismatch between the surface temperature T_i^0 and temperature just inside the system, T_i , denoted $\delta T_i = |T_i - T_i^0|$ [6]. Consequently, the *input* temperature difference, $\Delta T = T_2^0 - T_1^0$, can be decomposed into the two surface jumps, δT_1 , δT_2 , and the gradient contribution: $\Delta T = \int dx \nabla T + \delta T_1 + \delta T_2$. The jumps δT_i can be expressed as $\delta T_i = \eta \nabla T|_i$, where ∇T_i is the internal temperature gradient extrapolated to the surface i , and η is on the order of the mean free path at that temperature λ_i [7,8]. Hence we write $\delta T_i = \alpha \lambda_i \nabla T|_i$, where α is a constant corresponding to the efficacy of the boundary thermostats as they couple to the system. In this work, it will turn out that the boundary jumps become important in the near equilibrium regime, so that they are symmetric, $\delta T_1 \simeq \delta T_2$, and the gradient is constant, $\nabla T_i = \nabla T$. Thus we are led to the general near-equilibrium relationship, using the length L between the thermostats,

$$[2\alpha\lambda + L] \nabla T = \Delta T. \quad (1)$$

Seemingly simple, this relation can be used to derive many properties of the FPU model, and others in general.

In this letter we examine the FPU β Hamiltonian, $\tilde{H} = \sum_{k=1}^L \left[\frac{\tilde{p}_k^2}{2m} + \frac{1}{2}m\omega^2(\tilde{q}_{k+1} - \tilde{q}_k)^2 + \frac{\beta}{4}(\tilde{q}_{k+1} - \tilde{q}_k)^4 \right]$. Under the rescaling $\tilde{p}_k = p'_k \omega^2 \sqrt{m^3}$, $\tilde{q}_k = q'_k \omega \sqrt{m}$, we obtain the conventional form of the FPU β model,

$$H_\beta = \frac{1}{2} \sum_{k=1}^L \left[p_k'^2 + (q'_{k+1} - q'_k)^2 + \frac{\beta}{2}(q'_{k+1} - q'_k)^4 \right], \quad (2)$$

where $H_\beta = \tilde{H}/(m^2\omega^4)$. It is important to note that the temperature and the coupling are *not* independent parameters, but changing the temperature is equivalent to changing the coupling β . This can be seen by the further rescaling $p'_k = p_k/\sqrt{\beta}$, $q'_k = q_k/\sqrt{\beta}$, which leads to a unique, dimensionless, Hamiltonian $H \equiv H_{\beta=1} = \beta H_\beta$. Since we have rescaled the momenta $p_k'^2 = \beta p_k'^2$, the temperatures in the two formulations H and H_β are related by $T = \beta T'$. So the most general physics can be obtained by using H_β around a fixed temperature (for instance $T' = 1$) but with different couplings β , or by using H at various temperatures T . In this study we use H and probe temperatures from 10^{-4} to 10^4 , where $T_k = \langle p_k'^2 \rangle$ (ideal gas thermometer), using L sites and either free ($q_0 = q_1$, $q_L = q_{L+1}$) or fixed

($q_1 = q_L = 0$) boundary conditions. Perhaps surprisingly, these conditions have an effect on the measured transport properties.

Heat flow is generated when thermostats are coupled to the boundaries of the system. The system evolves according to Hamilton's equations of motion except at the boundaries, where we use Nosé-Hoover (NH) thermostats [9] or demons [10] (see [8], Eqs. (3)). The NH thermostats are observed not to thermalize the boundaries for large temperature gradients, a problem particularly acute for small lattices. The demons, on the other hand, do not suffer from this problem and hence provide a resolution to the problem recently studied in [11]. We have considered a range of coupling strengths as well as thermostatting one or more sites on each edge. Irrespective of the form of the boundary thermostats, we note that their introduction breaks global momentum conservation, $\dot{P}_{tot} \neq 0$, while it is conserved on average; $\langle \dot{P}_{tot} \rangle = 0$. The equations of motion, on the other hand, are still invariant with respect to the translations $q_k \rightarrow q_k + c$ for free or periodic boundary conditions, where c is an arbitrary constant. This disparity arises from the fact the the equations of motion for the whole system are no longer Hamiltonian.

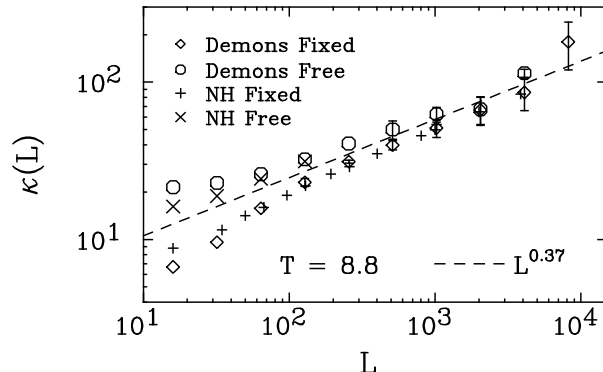


FIG. 1. Size dependence of the thermal conductivity of the FPU model for free or fixed boundary conditions with different thermostats. The Nosé-Hoover thermostats do not thermalize the boundaries for small L and hence their results deviate from those of the demons. $L^{0.37}$ behavior will be discussed along with Fig. 2.

The definition of heat current J depends on the form of the discrete gradient in the Hamiltonian and continuity equations. For instance, we may choose $h_k = p_k^2/2 + U(q_{k+1} - q_k)$ (where $H = \sum_k h_k$, $U(x) = x^2/2 + x^4/4$) and $\dot{h}_k + J_{k+1} - J_k = 0$, leading to the consistent form $J_k = -p_k U'(q_k - q_{k-1})$. Regardless of the form chosen, the measurement of J is the same. We then use Fourier's law, $J = -\kappa(T, L)\nabla T$, to obtain κ . In Fig. 1 (NH-fixed), we reproduce the analysis of [5], plotting κ using the boundary temperatures $(T_1^0, T_2^0) = (2.4, 15.2)$ to obtain $\kappa(8.8, L)$ and compare this to the results obtained using demons and also the free boundary condition results using the same (T_1^0, T_2^0) . This figure raises several significant points. First, the NH results do not thermalize the boundaries for smaller L , which accounts for the disagreement with the demon results. There is also a clear difference between the fixed or free boundaries. Free boundary conditions are found to result in the diffusion of the *entire* system in a Brownian manner: $\langle q^2 \rangle \sim t$, an essential difference. The differences in κ disappear as we increase the system size since the temperature gradients become small and we reach the near equilibrium regime. For small L , while $\nabla T \sim \text{constant}$, the system does not obey Fourier's law. We return to this in Fig. 4 below. Consequently, referring to these points as κ is not entirely correct.

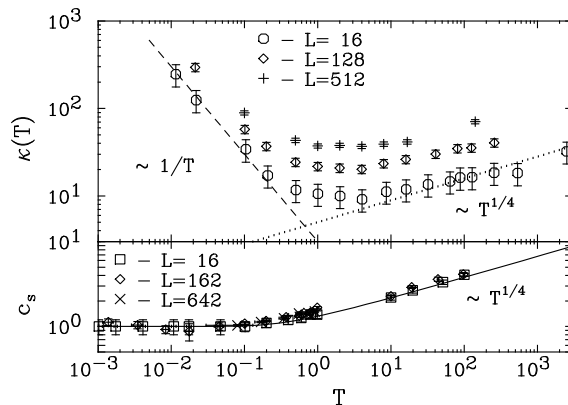


FIG. 2. (Top) T and L dependence of κ . One can see two regimes. For large T , there is an approximate $T^{1/4}$ behavior which can be understood from scaling arguments. For low T , a $1/T$ dependence which arises due to the weak coupling limit. The region where $T \sim 10$ has κ largely independent of T , so that Fourier's law can be strongly violated while the temperature profiles remain linear. This region was studied in [5] and Fig. 1. (Bottom) Speed of sound compared to expectations from soliton kinetic energy.

In Fig. 2 (top), we plot the T dependence of κ over 6 orders of magnitude for selected lattice sizes L with the fixed boundary conditions. To obtain these results, we first verified that Fourier's law $J = -\kappa(T, L)\nabla T$ is satisfied, by plotting J versus ∇T for various gradients. Only then, can we extract the conductivity κ correctly. The dotted and dashed lines represent the behavior we expect from the following arguments: At high T , the quartic term for q_k in the Hamiltonian H dominates over the quadratic term in q_k , as can be seen from the virial theorem, for instance. Therefore, in this asymptotic region, the Hamiltonian has the scaling property, $H/T = H'/T'$ under the rescalings $p_k = (T/T')^{1/2}p'_k$, $q_k = (T/T')^{1/4}q'_k$. In other words, the physics at different temperatures is related by simple kinematical rescalings. Applying this rescaling to the thermal conductivity, we derive $\kappa = -\langle J \rangle / \nabla T = (T/T')^{1/4}\kappa'$, which well describes the behavior $\kappa \sim T^{1/4}$ ($T \gg 1$) we have obtained.

The low temperature limit can be viewed as the weak coupling limit ($\beta \ll 1$) of H_β . Near the harmonic limit, we expect (and verify) the speed of sound c_s and heat capacity C_V to be unity. Hence kinetic theory suggests that $\kappa \sim \lambda$, where λ is the mean free path. The mean free path in this limit is on order of $\lambda \sim 1/\beta$ [12], so that $\kappa \sim 1/T$. We also find that the size dependence of κ has a power law behavior that is independent of the temperature, which is consistent with the previous results [13,4]. Consequently, we expect and find

$$\kappa \simeq \begin{cases} 1.2L^\delta T^{-1} & (T \lesssim 0.1) \\ 2L^\delta T^{1/4} & (T \gtrsim 50) \end{cases}, \quad \delta = 0.37(3). \quad (3)$$

This provides a much more global picture of heat transport in the FPU model than previously known.

The excitations in the FPU model are known to be solitonic [2,14]. The 'sound speed' c_s can be measured by examining how an initial perturbation in the center of the system propagates, as a function of lattice size L and temperature T . In Fig. 2 (bottom) we plot this together with the velocity behavior suggested from solitons, namely, $2T = c_s^3 \sqrt{c_s^2 - 1}$ [14]. The agreement is quite good aside from a weak L dependence which is not described by this approach.

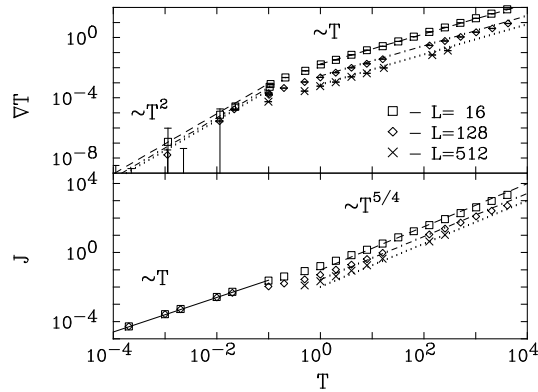


FIG. 3. Behavior of ∇T and J as a function of T compared to expected behaviors. Solitons propagate freely below $T_c \sim L^{1-\delta}$.

Consider now some consequences of Eq. (1). Kinetic theory indicates that $\kappa = \lambda c_s C_v$. Since $C_v \sim 1$ for all temperatures we measured, we have $\lambda \sim \kappa/c_s$. Hence, at low T , $\lambda \sim 1/T$, and the boundary jumps eventually dominate the thermal profile. The transition to this regime occurs when $L \sim 2\alpha\lambda = 2\alpha\kappa$ (we show below that $\alpha \sim 1$), or using Eq. (3), $T_c \sim 2L^{1-\delta}$. To delineate this behavior, we study the system at various central temperatures, T , with fixed relative differences $\Delta T/T \equiv r = 0.4$ in Fig. 3. For $T < T_c$, boundary jumps dominate Eq. (1), so that $J = \Delta T/(2\alpha) = (r/2\alpha)T \sim T/4$. Notice here that in this regime, J should be independent of L . This is indeed observed in Fig. 3 (bottom). The transition also is characterized by $\lambda \gtrsim L$, which means that excitations (solitons) now move freely across the system without interaction. This indicates the onset of the harmonic limit which is characterized by a flat temperature profile. We can use Eq. (1) to compute how fast we approach the harmonic limit: $\nabla T = (r/2\alpha\kappa)T = 0.2T^2L^{-\delta}$. Hence the system approaches the harmonic limit like T^2 . We have explicitly measured this behavior for several L and confirm it.

A frequently used argument surmises that for fixed boundary temperatures, the behavior of $\kappa(T, L)$ can be obtained from the behavior of J by assuming that ∇T scales like $1/L$ (see for example [15,5]). Our results demonstrate that such an argument in general is not applicable due to the presence of boundary jumps which cannot be ignored. It should be emphasized that the importance of jumps is unrelated to the absence of a bulk limit [8].

At higher temperatures, boundary jumps compete with the heat flow inside. Here c_s and κ both behave at $T^{1/4}$, so that λ is independent of T . Consequently, $\nabla T = r/(2\alpha\lambda + L)T = [0.4/(L + 3L^\delta)]T$ and $J = -\kappa\nabla T = [0.8/(L^{1-\delta} + 3)]T^{5/4}$. In Fig. 3, we show both ∇T and J as a function of T and see that the predicted behavior is consistent with measurements. The agreement includes not only the power law, but the prefactors as well, both for low and high T .

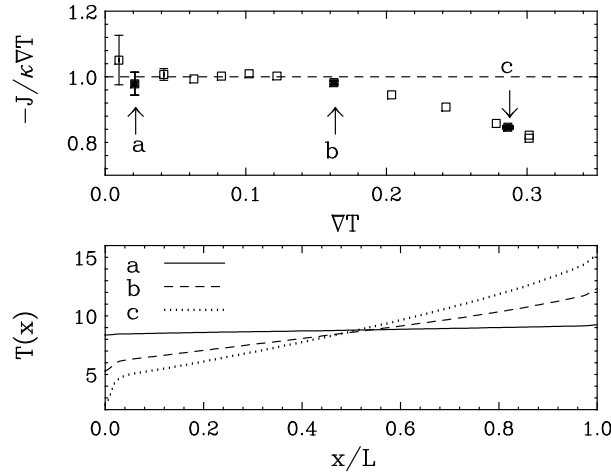


FIG. 4. (Top) Violation of Fourier's Law, $-J/\kappa\nabla T$, as a function of ∇T , showing departure from Fourier's law (dashes) at larger gradients. (Bottom) Temperature profiles for the three points indicated in the top figure. One can see that the profile has a fairly constant gradient in spite of the 20% violation of Fourier's law in (c).

Recently we have derived a formula for the temperature profile $T(x)$ in models where $\kappa(T)$ displays power law behavior, $\kappa \simeq \text{const.}/T^\gamma$, in the temperature range of interest [8,3]: $T(x) = T_1[1 - (1 - (T_2/T_1)^{1-\gamma})x/L]^{1/(1-\gamma)}$. In the present study, in looking at temperatures near $T=8.8$ in Fig. 2, κ is nearly *temperature independent* over more than a decade in temperature. Hence we expect $T(x) = T_1 + (T_2 - T_1)x/L + \mathcal{O}(\gamma)$ to develop almost no curvature for very large gradients, and hence the shape of $\nabla T(x)$ is *not* a good measure of the validity of Fourier's law. In Fig. 4 we plot $-J/\kappa\nabla T$ as a function of the measured ∇T . The dashed line represent the expected result when Fourier's law holds. One can see that as the gradient increases, noticeable systematic violations of Fourier's law develop. For the selected points, we plot the temperature profiles in Fig. 4 (bottom), demonstrating the nearly linear behavior. Similar behavior is also seen at higher temperatures, since $\kappa \sim T^{1/4}$ is a weak power law. Hence in contrast the the ϕ^4 model, where noticeable curvature in $T(x)$ develops when Fourier's law is broken [3], the FPU model demonstrates that *nearly constant temperature gradients do not imply Fourier heat flow*. It should be noted that one will underestimate the thermal conductivity if the Fourier's law is applied in this regime to obtain the conductivity.

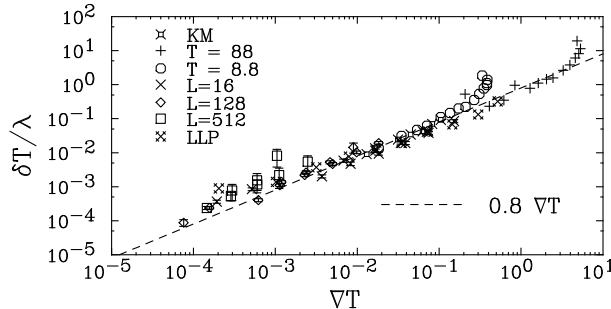


FIG. 5. Quantitative study of boundary jumps δT in our study, normalized by the mean free path λ , allow the determination of α . The results from previous stochastic (KM) and dynamic (LLP) studies have been rescaled and are also shown. One can see that over an extremely large range in jumps and gradients, a simple scaling behavior exists.

In order to compute the coefficient α , we must analyze the behavior of the boundary jumps $\delta T/\lambda$ as a function of ∇T . In Fig. 5, we combine results from various lattice sizes and temperatures, as well as from stochastic boundary conditions (see for instance Figs. 1 in ref. [13] and 2-4 in ref. [4]). In Fig. 5, we plot $\delta T/\lambda$ and see that this behaves as ∇T . In addition we show the behavior extracted from stochastic boundary conditions as well as from previous calculations in the FPU, which are quite consistent with our results. We then extract the parameter $\alpha = 0.8(1)$ for the demons. A necessary consequence is that the temperature profiles cannot be shape invariant in the way discussed in [5]. While the same scaling is found for different thermostats, the coefficient α can be different. For NH demons (LLP) used in [5,13], $\alpha_{NH} = 2.0(3)$ and for stochastic boundary conditions (KM) in [4], it is much larger, $\alpha_S = 40(6)$, as evidenced in the large boundary jumps seen in [4].

We have seen that the interplay of surface and volume effects in Eq. (1) can be used to understand transport properties. Since the conductivity in this model has no bulk limit, the transport depends not only on the method used to thermalize the boundaries, but also on the boundary conditions themselves. Nevertheless, one can understand the temperature dependence at low and high temperatures. We have been able to map out $\kappa(T, L)$ and provide an analytical understanding in the asymptotic regimes. The FPU model also provides an example of a theory where Fourier's law breaks down, but the temperature profile retains a nearly constant gradient. This can be understood in terms of the weak temperature dependence of the conductivity. The boundary jumps also display a very systematic behavior over many decades in ∇T , independent of the types of thermostats (dynamics or stochastic) or of the lattice size. This dependence on ∇T also shows that the temperature profiles cannot be shape invariant unless the boundary jumps are explicitly taken into account.

We acknowledge support from grants at Keio University and DOE grant DE-FG02-91ER40608.

^a E-mail: ken@phys-h.keio.ac.jp

^b E-mail: dimitri@nst.physics.yale.edu

- [1] C. Giadina, R. Livi, A. Politi, M. Vassalli, *Phys. Rev. Lett.* **84** 2144 (2000); T. Prosen, D. Campbell, *Phys. Rev. Lett.* **84** (2000) 2857; O.V. Gendelman, A.V. Savin, *Phys. Rev. Lett.* **84** (2000) 2381; T. Hatano, *Phys. Rev.* **E59** R1 (1999).
- [2] B. Hu, B. Li, H. Zhao, *Phys. Rev.* **E61** 3828 (1999).
- [3] K. Aoki, D. Kusnezov, *Phys. Lett.* **B477** (2000) 348
- [4] H. Kaburaki, M. Machida, *Phys. Lett.* **A181** (1993) 85.
- [5] S. Lepri, R. Livi, A. Politi, *Phys. Rev. Lett.* **78** (1997) 1896
- [6] For simulation results, see, T. Tanenbaum, G. Ciccotti, R. Gallico, *Phys. Rev.* **A25** (1982) 2778; T. Prosen, M. Robnik, *J. Phys. A* **25** (1992) 3449; M.J. Gillian, R.W. Holloway, *J. Phys.* **C18** (1985) 5705; D.K. Bhattacharya, G.C. Lie, *Phys. Rev.* **A43** (1991) 761. For experimental results, see *e.g.*, H. Ziebland, in *Thermal Conductivity*, ed. R. P. Tye, (Academic, New York, 1969), Vol 2.
- [7] E. M. Lifshits, L.P. Pitaevskii, *Physical Kinetics*, (Pergamon Press, New York, 1981).
- [8] K. Aoki and D. Kusnezov, *Phys. Lett.* **A265** (2000) 250.
- [9] S. Nosé, *J. Chem. Phys.* **81**, 511 (1984); *Mol. Phys.* **52** (1984) 255 ; W. G. Hoover, *Phys. Rev. A* **31** (1985) 1695; W.G.Hoover, *Computational Statistical Mechanics* (Elsevier, Amsterdam, 1991).
- [10] D. Kusnezov, A. Bulgac, W. Bauer, *Ann. Phys.* **204** (1990) 155; D. Kusnezov, J. Sloan, *Nucl. Phys.* **B409** (1993) 635; D. Kusnezov, *Phys. Lett.* **166A** 315 (1992).
- [11] A. Phillipov, B. Hu, B. Li, A. Zeltser, *J. Phys. A: Math. Gen.* **31** (1998) 7719.
- [12] See, for instance, N.W. Ashcroft, D.N. Mermin, “*Solid State Physics*”, Harcourt College Publishers (1976)
- [13] S. Lepri, R. Livi, A. Politi, *Physica* **D119** (1998) 140
- [14] F. Zhang, D.J. Isbister, D.J. Evans, *Phys. Rev.* **E61** (2000) 3541.
- [15] G. Tsironis, A. R. Bishop, A.V. Savin, A.V. Zolotaryuk, *Phys. Rev.* **E60** (1999) 6610.